

A Three-loop Neutrino Model with Leptoquark Triplet Scalars

Kingman Cheung,^{1,2,3,*} Takaaki Nomura,^{4,†} and Hiroshi Okada^{1,‡}

¹*Physics Division, National Center for Theoretical Sciences, Hsinchu, Taiwan 300*

²*Department of Physics, National Tsing Hua University, Hsinchu 300, Taiwan*

³*Division of Quantum Phases and Devices, School of Physics,*

Konkuk University, Seoul 143-701, Republic of Korea

⁴*School of Physics, KIAS, Seoul 130-722, Korea*

(Dated: March 10, 2022)

Abstract

We propose a three-loop neutrino mass model with a few leptoquark scalars in $SU(2)_L$ -triplet form, through which we can explain the anomaly of $B \rightarrow K^{(*)}\mu^+\mu^-$, a sizable muon $g - 2$ and a bosonic dark matter candidate, and at the same time satisfying all the constraints from lepton flavor violations. We perform global numerical analyses and show the allowed regions, in which we find somewhat restricted parameter space, such as the mass of dark matter candidate and various components of the Yukawa couplings in the model.

Keywords:

*Electronic address: cheung@phys.nthu.edu.tw

†Electronic address: nomura@kias.re.kr

‡Electronic address: macokada3hiroshi@cts.nthu.edu.tw

I. INTRODUCTION

Recently, there was an 2.6σ anomaly in lepton-universality violation in the ratio $R_K \equiv B(B \rightarrow K\mu\mu)/B(B \rightarrow K\ell\ell) = 0.745^{+0.090}_{-0.074} \pm 0.036$ by the LHCb Collaboration [1]. In addition, sizable deviations were observed in angular distributions of $B \rightarrow K^*\mu\mu$ [2]. The results can be interpreted by a large negative contribution to the Wilson coefficient C_9 of the semileptonic operator O_9 , and also contributions to other Wilson coefficients, in particular to C'_9 [3–6].

The discrepancy between the theoretical prediction and experimental value on the muon anomalous magnetic dipole moment has been a long-standing problem, which stands at 3.6σ level with the deviation from the SM prediction at [7].

$$\Delta a_\mu = a_\mu^{\text{exp}} - a_\mu^{\text{SM}} = 288(63)(49) \times 10^{-11}.$$

If one insists on fulfilling the muon $g - 2$ within $1\sigma - 2\sigma$ of the experimental value in any models, it puts a strong constraint on the parameter space. For example, it requires a relatively light spectrum in the supersymmetric particles in the MSSM in order to bring the prediction to be within $1\sigma - 2\sigma$ of the experimental value. A number of leptoquark models have been proposed to solve the $B \rightarrow K^{(*)}\mu\mu$ anomaly, but however it is very hard to satisfy simultaneously the muon $g - 2$: see for example Ref. [8].

In this work, we propose a three-loop neutrino mass model with a few leptoquark scalars in $SU(2)_L$ -triplet form. We attempt to use the model to explain the anomaly of $B^{(*)} \rightarrow K\mu^+\mu^-$, to achieve a sizable muon $g - 2$, and to provide a bosonic dark matter candidate, and at the same time satisfying all the constraints from lepton flavor violations. The concrete model is based on the SM symmetry and a Z_2 symmetry as $SU(3)_C \times SU(2)_L \times U(1)_Y \times Z_2$. The model consists of the SM fields, 3 additional leptoquark triplet fields $\Delta_{1,2,3}^a$, and one colorless doublet scalar field η . These fields are assigned different Z_2 parities and hypercharges in such a way that each of the Yukawa-type couplings contributes to either neutrino mass, $B \rightarrow K^{(*)}\mu\mu$ anomaly, muon $g - 2$, or the dark matter interactions. In this way, although the model contains more parameter, it can however explain all the above anomalies. The achievements of the model can be summarized in the following.

1. The neutrino mass pattern and oscillation can be accommodated with the Yukawa

	Quarks			Leptons		Vector Fermions
	$Q_{L_i}^a$	$u_{R_i}^a$	$d_{R_i}^a$	L_{L_i}	e_{R_i}	L'_i
$SU(3)_C$	3	3	3	1	1	1
$SU(2)_L$	2	1	1	2	1	2
$U(1)_Y$	$\frac{1}{6}$	$\frac{2}{3}$	$-\frac{1}{3}$	$-\frac{1}{2}$	-1	$-\frac{1}{2}$
Z_2	+	+	+	+	+	−

TABLE I: Field contents of fermions and their charge assignments under $SU(3)_C \times SU(2)_L \times U(1)_Y \times Z_2$, where the superscript (subscript) index a (i) = 1 – 3 represents the color (flavor).

coupling terms f, g, h in three-loop diagrams ¹.

2. The Yukawa coupling term f can give useful contributions to the Wilson coefficients $C_{9,10}$ in such a way that it can explain successfully the $B \rightarrow K^{(*)}\mu\mu$ anomaly.
3. The muon $g - 2$ receives a large contribution from the Yukawa coupling term r . With some adjustment of the parameters a level of 10^{-9} is possible.
4. It provides a dark matter (DM) candidate η_R , the real part of the neutral component of the η field with correct relic density.
5. The model can satisfy all the existing constraints from the lepton-flavor violations (LFVs), meson mixings, and rare B decays.

This paper is organized as follows. In Sec. II, we describe the neutrino mass matrix and the solution to the anomaly in $b \rightarrow s\mu\bar{\mu}$. In Sec. III, we discuss various constraints of the model, including lepton-flavor violations, FCNC's, oblique parameters, and dark matter. In Sec. IV, we present the numerical analysis and allowed parameter space, followed by the discussion on collider phenomenology. Sec. IV is devoted for conclusions and discussion.

II. THE MODEL

In this section, we describe the model setup, derive the formulas for the active neutrino mass matrix, and calculate the contributions to $b \rightarrow s\mu\bar{\mu}$.

¹ See refs. [9–11] for representative three loop neutrino mass models

	Φ	η	Δ_1^a	Δ_2^a	Δ_3^a
$SU(3)_C$	1	1	3	$\bar{\mathbf{3}}$	$\bar{\mathbf{3}}$
$SU(2)_L$	2	2	3	3	3
$U(1)_Y$	$\frac{1}{2}$	$\frac{1}{2}$	$\frac{2}{3}$	$\frac{1}{3}$	$\frac{1}{3}$
Z_2	+	-	-	-	+

TABLE II: Field contents of bosons and their charge assignments under $SU(3)_C \times SU(2)_L \times U(1)_Y \times Z_2$, where the superscript index $a = 1 - 3$ represents the color.

A. Model setup

We show all the field contents and their charge assignments in Table I for the fermionic sector and in Table II for the bosonic sector.² Under this framework, the relevant part of the renormalizable Lagrangian and Higgs potential related to the neutrino masses are given by

$$\begin{aligned}
-\mathcal{L} = & y_{\ell_i} \bar{L}_{L_i} \Phi e_{R_i} + f_{ij} \bar{L}_{L_i} \Delta_3^\dagger (i\sigma_2) Q_{L_j}^c + g_{ij} \bar{L}'_{R_i} \Delta_1^\dagger Q_{L_j} + h_{ij} \bar{L}'_{L_i} \Delta_2^\dagger Q_{L_j}^c + r_{ij} \bar{L}'_{L_i} \eta e_{R_j} \\
& + M_i \bar{L}'_{L_i} L'_{R_i} - \lambda_0 \eta^\dagger \Delta_3 \Delta_1 \Phi^* - \lambda'_0 \eta^\dagger \Delta_3 \Delta_2^* \Phi - \lambda_5 (\eta^\dagger \Phi)^2 + \text{h.c.},
\end{aligned} \tag{II.1}$$

where we have defined $L' \equiv [N, E]^T$, σ_2 is the second Pauli matrix and we have abbreviated the trivial terms for the Higgs potential. The scalar fields can be parameterized as

$$\begin{aligned}
\Phi = \begin{bmatrix} 0 \\ \frac{v+\phi}{\sqrt{2}} \end{bmatrix}, \quad \eta = \begin{bmatrix} \eta^+ \\ \frac{\eta_R + i\eta_I}{\sqrt{2}} \end{bmatrix}, \quad \Delta_1 = \begin{bmatrix} \frac{\delta_{2/3}^{(1)}}{\sqrt{2}} & \delta_{5/3}^{(1)} \\ \delta_{-1/3}^{(1)} & -\frac{\delta_{2/3}^{(1)}}{\sqrt{2}} \end{bmatrix}, \\
\Delta_2 = \begin{bmatrix} \frac{\delta_{1/3}^{(2)}}{\sqrt{2}} & \delta_{4/3}^{(2)} \\ \delta_{-2/3}^{(2)} & -\frac{\delta_{1/3}^{(2)}}{\sqrt{2}} \end{bmatrix}, \quad \Delta_3 = \begin{bmatrix} \frac{\delta_{1/3}^{(3)}}{\sqrt{2}} & \delta_{4/3}^{(3)} \\ \delta_{-2/3}^{(3)} & -\frac{\delta_{1/3}^{(3)}}{\sqrt{2}} \end{bmatrix},
\end{aligned} \tag{II.2}$$

where the subscript next to the each field represents the electric charge of the field, $v = 246$ GeV, and Φ is written in the form after the Goldstone fields are abosorbed as the longitudinal components of W and Z bosons. Notice here that each of the components of Δ_3 and η is

² The same contents of the field are found in the systematic analysis in the last part of Table 3 of ref. [12].

in mass eigenstate, since there are no mixing terms that are assured by the Z_2 and $U(1)_Y$ symmetries. On the other hand, components of Δ_1 and Δ_2 can mix via $\Phi^*\Phi^*\Delta_1\Delta_2$ term. In the following analysis, we ignore such mixing effects assuming the relevant coupling is small.

Oblique parameters: Each of the mass components among Δ_i is strongly restricted by the oblique parameters. In order to evade such a strong constraint, we simply assume that each of the components should be of the same mass [13]. Thus, we define m_{Δ_i} as the mass for the components of Δ_i . On the other hand, each component of η cannot have the same mass, because the neutrino mass is proportional to the mass difference between the components of η , as you shall see later. Hence, we consider the oblique parameter constraints on η , which are characterized by ΔT and ΔS . Their formulae are given by [14]

$$\Delta T = \frac{F[\eta^\pm, \eta_I] + F[\eta^\pm, \eta_R] - F[\eta_I, \eta_R]}{32\pi^2\alpha_{em}v^2}, \quad \Delta S = \frac{1}{2\pi} \int_0^1 x(1-x) \ln \left[\frac{xm_{\eta_R}^2 + (1-x)m_{\eta_I}^2}{m_{\eta^\pm}^2} \right], \quad (\text{II.3})$$

where $\alpha_{em} \approx 1/137$ is the fine structure constant, and

$$F[a, b] = \frac{m_a^2 + m_b^2}{2} - \frac{m_a^2 m_b^2}{m_a^2 - m_b^2} \ln \left[\frac{m_a^2}{m_b^2} \right], \quad m_a \neq m_b. \quad (\text{II.4})$$

The experimental bounds are given by [7]

$$(0.05 - 0.09) \leq \Delta S \leq (0.05 + 0.09), \quad (0.08 - 0.07) \leq \Delta T \leq (0.08 + 0.07). \quad (\text{II.5})$$

We consider these constraints in the numerical analysis.

Active neutrino mass matrix: The neutrino mass matrix is induced at three-loop level as shown in Fig. 1, and its formula is generally given by

$$\mathcal{M}_{\nu_{ij}} = \mathcal{M}_{\nu_{ij}}^d + \mathcal{M}_{\nu_{ij}}^u + tr., \quad [\mathcal{M}_\nu^u = 2\mathcal{M}_\nu^d(d \rightarrow u, \delta_{1/3}^{(i)} \rightarrow \delta_{2/3}^{(i)})], \quad (\text{II.6})$$

$$\mathcal{M}_{\nu_{ab}}^d = \frac{3^2 \lambda_0 \lambda_0' (m_R^2 - m_I^2) v^2}{2\sqrt{2}(4\pi)^6 M_{max}^4} \sum_{(a,b,c)=1}^3 f_{ia} g_{ab}^T M_b h_{bc}^* f_{cj}^T F_{III}[r_{\Delta_1}, r_{\Delta_2}, r_{\Delta_3}, r_b, r_R, r_I, r_{d_c}, r_{d_a}], \quad (\text{II.7})$$

where we used the shorthand notation $m_{R/I} \equiv m_{\eta_{R/I}}$, and define $M_{\text{Max}} \equiv \text{Max}[M_b, m_{\Delta_i}, m_R, m_I]$, $r_f \equiv m_f^2/M_{\text{Max}}^2$, and the three-loop function F_{III} is given in the Appendix. Here we adopt an assumption $M_{max} = m_{\Delta_3}$, and require $1\text{TeV} \lesssim m_{\Delta_i}$ (which

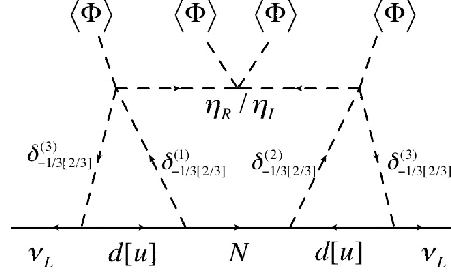


FIG. 1: Neutrino mass matrix at the three-loop level, where we have two kind of diagrams that are running up-quarks and down quarks inside the loop.

suggests $x_d, x_u \approx 0$), which is required by the direct bound on leptoquarks [13]. In this case, the neutrino mass matrix can be simplified as

$$\mathcal{M}_{\nu_{ij}} \approx \frac{3^3 \lambda_0 \lambda'_0 (m_R^2 - m_I^2) v^2}{2\sqrt{2}(4\pi)^6 m_{\Delta_3}^4} [f g^T (M F_{III}) h^* f^T]_{ij} + tr., \quad (\text{II.8})$$

where we have abbreviated the symbol of summation and the argument of F_{III} . Then we derive the Yukawa coupling in terms of the experimental values and the parameters by introducing an arbitrary anti-symmetric matrix with complex values A [15], that is $A^T + A = 0$, as follows:

$$g = \frac{1}{2} R^{-1} (h^\dagger)^{-1} [f^{-1} V_{MNS} D_\nu V_{MNS}^T (f^T)^{-1} + A]^T, \quad (\text{II.9})$$

or

$$h = \frac{1}{2} R^{*-1} (g^\dagger)^{-1} [f^{-1} V_{MNS} D_\nu V_{MNS}^T (f^T)^{-1} + A]^*, \quad (\text{II.10})$$

where we shall adopt the former formula in the numerical analysis below, and we define $D_\nu \equiv V_{MNS}^T \mathcal{M}_\nu V_{MNS}$ and parametrize as

$$R = \frac{3^3 \lambda_0 \lambda'_0 (m_R^2 - m_I^2) v^2 M F_{III}}{2\sqrt{2}(4\pi)^6 m_{\Delta_3}^4}, \quad A \equiv \begin{bmatrix} 0 & a_{12} & a_{13} \\ -a_{12} & 0 & a_{23} \\ -a_{13} & -a_{23} & 0 \end{bmatrix}. \quad (\text{II.11})$$

Here we assume one massless neutrino (with normal ordering) in the numerical analysis below.

On the term f : The new physics contributions to account for the $B \rightarrow K^{(*)} \mu \mu$ anomaly [2] can be interpreted as the shifts in the Wilson coefficients $C_{9,10}$. In our model, the relevant

Wilson coefficients can be calculated as follows [13]:

$$(C_9)^{\mu\mu} = -(C_{10})^{\mu\mu} = -\frac{1}{C_{\text{SM}}} \frac{f_{b\mu} f_{s\mu}}{4m_{\Delta_3}^2}, \quad C_{\text{SM}} \equiv \frac{V_{tb} V_{ts}^* G_F \alpha_{\text{em}}}{\sqrt{2}\pi}, \quad (\text{II.12})$$

where $m_{\Delta_3} \equiv m_{\delta_{4/3}^{(3)}}$, $G_F \approx 1.17 \times 10^{-5} \text{ GeV}^{-2}$ is the Fermi constant. We can then compare them to the *best-fit values* of $C_{9,10}$ from a global analysis based on the LHCb data in Ref. [3] as

$$C_9 = -C_{10} : -0.68. \quad (\text{II.13})$$

Here we also have to work within the $-0.75 \lesssim C_9 \lesssim -0.35$ in order to satisfy the the LHCb measurement of $R_K = B(B^+ \rightarrow K^+ \mu^+ \mu^-) / B(B^+ \rightarrow K^+ e^+ e^-) = 0.745_{-0.074}^{+0.090} \pm 0.036$, which shows a 2.6σ deviation from the SM prediction [13]. *Notice here that various constraints arising from the f term include $B_{d/s} \rightarrow \ell^+ \ell^-$, $\ell_i \rightarrow \ell_j \gamma$, which were given in Refs. [13] and [8], and we consider these constraints in the current numerical analysis. Although the muon $g-2$ is also induced from this term, the typical order is $10^{-12} \sim 10^{-13}$ with a negative sign [13]. Thus, we neglect this contribution to the muon $g-2$.*

On the terms g and h : The main constraint on g and h comes from $B(b \rightarrow s\gamma)$. The partial decay width for $b \rightarrow s\gamma$ is given by

$$\Gamma(b \rightarrow s\gamma) \approx \frac{3\alpha_{\text{em}} m_b^5}{4(4\pi)^4} \left| \frac{g_{2a}^\dagger g_{a3}}{2} F_{bs\gamma}[\delta_{2/3}^{(1)}, a] - h_{3a}^\dagger h_{a2} \left(\frac{5}{3} F_{bs\gamma}[a, \delta_{1/3}^{(2)}] + F_{bs\gamma}[\delta_{1/3}^{(2)}, a] \right) \right|^2, \quad (\text{II.14})$$

$$F_{bs\gamma}[a, b] = \frac{2m_a^6 + 3m_a^4 m_b^2 - 6m_a^2 m_b^4 + m_b^6 + 12m_a^4 m_b^2 \ln[m_b/m_a]}{12(m_a^2 - m_b^2)^4}, \quad (\text{II.15})$$

then the branching ratio and its experimental bound [16] are given by

$$B(b \rightarrow s\gamma) \approx \frac{\Gamma(b \rightarrow s\gamma)}{\Gamma_{\text{tot.}}} \lesssim 3.29 \times 10^{-4}, \quad (\text{II.16})$$

where $\Gamma_{\text{tot.}} \approx 4.02 \times 10^{-13} \text{ GeV}$ is the total decay width of the bottom quark. In our numerical analysis, we consider this constraint only for the g and h terms.

On the term r : This term is very important in our model because it can induce a large contribution to the muon $g-2$ and explain the relic density of dark matter (DM) if we assume the η_R to be the DM candidate. First of all, let us consider the LFVs processes, $\ell_a \rightarrow \ell_b \gamma$, via one-loop diagrams. The branching ratio is given by

$$B(\ell_a \rightarrow \ell_b \gamma) = \frac{48\pi^3 C_{ab} \alpha_{\text{em}}}{G_F^2 m_a^2} (|(a_R)_{ab}|^2 + |(a_L)_{ab}|^2), \quad (\text{II.17})$$

where $m_{a(b)}$ is the mass for the charged-lepton eigenstate, $C_{ab} \approx (1, 0.1784, 0.1736)$ for $(a, b) = (2, 1), (3, 1), (3, 2)$, and $a_{L(R)}$ is simply given by

$$(a_{L(R)})_{ab} \approx \sum_{i=1}^3 \frac{r_{bi}^\dagger r_{ia} m_a}{(4\pi)^2} \left(F_{l\bar{f}v}^{L(R)}[N_i, \eta^\pm] - \frac{1}{2} F_{l\bar{f}v}^{L(R)}[\eta_I, E_i] - \frac{1}{2} F_{l\bar{f}v}^{L(R)}[\eta_R, E_i] \right), \quad (\text{II.18})$$

$$F_{l\bar{f}v}^L[a, b] = \frac{m_a^4 + 2m_a^2 m_b^2 + 2m_b^2(m_a^2 + m_b^2) \ln\left(\frac{m_b^2}{m_a^2 + m_b^2}\right)}{6m_a^6}, \quad F_{l\bar{f}v}^R[a, b] = \frac{m_a^2 + m_b^2 \ln\left(\frac{m_b^2}{m_a^2 + m_b^2}\right)}{6m_a^4}, \quad (\text{II.19})$$

where the mass of $E(N)_a$ is defined by $M_{E(N)_a}$. Current experimental upper bounds are given by [17, 18]

$$B(\mu \rightarrow e\gamma) \leq 4.2 \times 10^{-13}, \quad B(\tau \rightarrow \mu\gamma) \leq 4.4 \times 10^{-8}, \quad B(\tau \rightarrow e\gamma) \leq 3.3 \times 10^{-8}. \quad (\text{II.20})$$

Muon $g-2$: The muon anomalous magnetic moment is simply given by $\Delta a_\mu \approx -m_\mu[a_L + a_R]_{22}$ in Eq. (II.19). Experimentally, it has been measured with a high precision, and its deviation from the SM prediction is $\Delta a_\mu = \mathcal{O}(10^{-9})$ [19]. It would be worth mentioning a new contribution to the leptonic decay of the Z boson. In our case, the Z boson can decay into a pair of charged leptons with a correction at one-loop level, and it is proportional to the Yukawa couplings related to the muon $g-2$. Therefore it can be enhanced due to the large Yukawa couplings. However, we have checked that this mode is within the experimental bound: $B(Z \rightarrow \ell\bar{\ell}) \lesssim 3 \times 10^{-2}$.

$Q - \bar{Q}$ mixing: The forms of $K^0 - \bar{K}^0$, $B_d^0 - \bar{B}_d^0$, and $D^0 - \bar{D}^0$ mixings are, respectively, given by

$$\begin{aligned} \Delta m_K \approx & \frac{1}{(4\pi)^2} \sum_{i,j=1}^3 \left[g_{i2} g_{1i}^\dagger g_{1j}^\dagger g_{j2} \left(F_{box}^K[N_i, N_j, \delta_{1/3}^{(1)}] + \frac{F_{box}^K[E_i, E_j, \delta_{2/3}^{(1)}]}{4} \right) \right. \\ & + f_{i1}^\dagger f_{2i} f_{2j} f_{j1}^\dagger \left(F_{box}^K[\ell_i, \ell_j, \delta_{4/3}^{(3)}] + \frac{F_{box}^K[\nu_i, \nu_j, \delta_{1/3}]}{4} \right) \\ & \left. + h_{i1}^\dagger h_{2i} h_{2j} h_{j1}^\dagger \left(F_{box}^K[E_i, E_j, \delta_{4/3}^{(2)}] + \frac{F_{box}^K[N_i, N_j, \delta_{1/3}^{(2)}]}{4} \right) \right] \lesssim 3.48 \times 10^{-15} [\text{GeV}], \end{aligned} \quad (\text{II.21})$$

$$\begin{aligned} \Delta m_{B_d} \approx & \frac{1}{(4\pi)^2} \sum_{i,j=1}^3 \left[g_{i3} g_{1i}^\dagger g_{1j}^\dagger g_{j3} \left(F_{box}^B[N_i, N_j, \delta_{1/3}^{(1)}] + \frac{F_{box}^B[E_i, E_j, \delta_{2/3}^{(1)}]}{4} \right) \right. \\ & + f_{i3}^\dagger f_{1i} f_{1j} f_{j3}^\dagger \left(F_{box}^B[\ell_i, \ell_j, \delta_{4/3}^{(3)}] + \frac{F_{box}^B[\nu_i, \nu_j, \delta_{1/3}]}{4} \right) \\ & \left. + h_{i3}^\dagger h_{1i} h_{1j} h_{j3}^\dagger \left(F_{box}^B[E_i, E_j, \delta_{4/3}^{(2)}] + \frac{F_{box}^B[N_i, N_j, \delta_{1/3}^{(2)}]}{4} \right) \right] \lesssim 3.36 \times 10^{-13} [\text{GeV}], \end{aligned} \quad (\text{II.22})$$

$$\begin{aligned} \Delta m_D \approx & \frac{1}{(4\pi)^2} \sum_{i,j=1}^3 \left[g_{i2} g_{1i}^\dagger g_{1j}^\dagger g_{j2} \left(F_{box}^D[E_i, E_j, \delta_{5/3}^{(1)}] + \frac{F_{box}^D[N_i, N_j, \delta_{2/3}^{(1)}]}{4} \right) \right. \\ & + f_{i1}^\dagger f_{2i} f_{2j} f_{j1}^\dagger \left(F_{box}^D[\ell_i, \ell_j, \delta_{4/3}^{(3)}] + \frac{F_{box}^D[\nu_i, \nu_j, \delta_{1/3}]}{4} \right) \\ & \left. + h_{i1}^\dagger h_{2i} h_{2j} h_{j1}^\dagger \left(F_{box}^D[N_i, N_j, \delta_{2/3}^{(2)}] + \frac{F_{box}^D[E_i, E_j, \delta_{1/3}^{(2)}]}{4} \right) \right] \lesssim 6.25 \times 10^{-15} [\text{GeV}], \end{aligned} \quad (\text{II.23})$$

$$F_{box}^Q(x, y, z) = \frac{5m_Q f_Q^2}{24} \left(\frac{m_Q}{m_{q_1} + m_{q_2}} \right)^2 \int \frac{\delta(1 - a - b - c - d) da db dc dd}{[am_x^2 + bm_y^2 + (c + d)m_z^2]^2}, \quad (\text{II.24})$$

where (q_1, q_2) are respectively (d, s) for K , (b, d) for B , and (u, c) for D . Each of the last inequalities in Eqs.(II.21 – II.23) represents the upper bound on the corresponding experimental value [7]. Here we used $f_K \approx 0.156$ GeV, $f_B \approx 0.191$ GeV, $m_K \approx 0.498$ GeV, and $m_B \approx 5.280$ GeV.³

Dark Matter: Here we identify η_R as the DM candidate, and denote its mass by $m_R \equiv M_X$.

Direct detection: We have a Higgs portal contribution to the DM-nucleon scattering process,

³ Since we assume that one of the neutrino masses to be zero with normal ordering that leads to the first column in g to be almost zero, i.e., $(g)_{11,12,13} \approx 0$, and so these constraints can easily be evaded.

which is constrained by direct detection search such as the LUX experiment [20]. Its spin independent cross section is simply given by [21]

$$\sigma_N \approx 2.12 \times 10^{-42} \times \left(\frac{(\lambda_3 + \lambda_4 + 2\lambda_5)v}{M_X} \right)^2 [\text{cm}]^2, \quad (\text{II.25})$$

where λ_3 and λ_4 are quartic couplings proportional to $(\eta^\dagger \eta)(\Phi^\dagger \Phi)$ and $(\eta^\dagger \Phi)(\Phi^\dagger \eta)$, respectively. The current experimental minimal bound is $\sigma_N \lesssim 2 \times 10^{-46} \text{ cm}^2$ at $M_X \approx 50 \text{ GeV}$. Once we apply this bound on our model, we obtain $\lambda_3 + \lambda_4 + 2\lambda_5 \lesssim 2 \times 10^{-3}$. Hence we assume that all the Higgs couplings are small enough to satisfy the constraint, and we neglect DM annihilation modes via Higgs portal in estimating the relic density below. Notice here that photon and Z boson fields transform as $V_\mu \rightarrow -V^\mu$ under charge-parity (CP) conjugation, while X is CP -even. Thus $X - X - \gamma(Z)$ couplings are not allowed because they violate the CP invariance.

Relic density: We consider parameter region in which the DM annihilation cross section is d -wave dominant and the dark matter particles annihilate into a pair of charged-leptons, via the process $\eta_R \eta_R \rightarrow \ell_i \bar{\ell}_j$ with an E_a exchange. Notice that there exist annihilation modes such as $\eta_R \eta_R \rightarrow W^+ W^- / 2Z$ arising from the kinetic term. These modes require a DM mass heavier than at least 500 GeV [22] in order to obtain the correct relic density where coannihilation processes should be included. This case is, however, not in favor of explaining the muon $g - 2$ anomaly. *Thus we assume that $M_X \lesssim 80 \text{ GeV}$ and $\eta_R \eta_R \rightarrow W^+ W^- / 2Z$ processes are not kinematically allowed.*⁴ Then the relic density is simply given by

$$\Omega h^2 \approx \frac{1.70 \times 10^7 x_f^3}{\sqrt{g^*} M_P d_{\text{eff}} [\text{GeV}]}, \quad d_{\text{eff}} \approx \sum_{(i,j,a)=1}^3 \frac{|r_{ia} r_{a,j}^\dagger|^2 M_X^6}{120\pi (M_{E_a}^2 + M_X^2)^4}, \quad (\text{II.26})$$

where $g^* \approx 100$, $M_P \approx 1.22 \times 10^{19}$, $x_f \approx 25$. In our numerical analysis below, we use the current experimental range for the relic density: $0.11 \leq \Omega h^2 \leq 0.13$ [23].

⁴ Here we impose the condition $m_Z/2 (\approx 41 \text{ GeV}) \lesssim m_R + m_I$ to forbid the invisible decay of Z boson in our numerical analysis, although the invisible decay of SM Higgs is automatically suppressed in the limit of zero couplings in the Higgs potential.

III. NUMERICAL ANALYSIS

As a first step, we perform the numerical analysis on the r term since this term is independent of the other parameters. We prepare *25 million* random sampling points for the relevant input parameters as follows:

$$\begin{aligned} M_X &\in [1, 80]\text{GeV}, \quad m_I \approx m_{\eta^\pm} \in [1.1 \times M_X, 200]\text{GeV}, \\ M_1 &\in [1.1 \times M_X, 330]\text{GeV}, \quad M_2 \in [M_1, 600]\text{GeV}, \quad M_3 \in [M_2, 700]\text{GeV}, \\ r' &\in [-9, \ln(4\pi)], \end{aligned} \tag{III.1}$$

where we define $M_i \equiv M_{E_i} = M_{N_i} (i = 1 - 3)$, $r_{ij} \equiv (\pm 1) \times 10^{r'_{ij}}$ and the lower mass bound $1.1 \times M_X$ is expected to forbid the coannihilation processes. Under such parameter ranges, we have found 246 allowed points, which are shown in Fig. 2 satisfying all the constraints including LFVs, oblique parameters, and invisible decay of Z boson, as discussed before. The left panel shows the allowed region to be

$$25[\text{GeV}] \lesssim M_X \lesssim 80[\text{GeV}], \quad 70[\text{GeV}] \lesssim m_{\eta^\pm} \lesssim 140[\text{GeV}], \tag{III.2}$$

where the lower bound of η^\pm comes from the LEP experiment [24, 25]. The right panel shows the correlation of r_{12} versus Δa_μ , where r_{12} is the most relevant parameter to obtain the sizable muon $g - 2$ and correct relic density of the DM. It suggests that a rather small r_{12} is possible to achieve the range $10^{-9} \leq \Delta a_\mu \leq 2 \times 10^{-9}$, but we need a large r_{12} for the range $2 \times 10^{-9} < \Delta a_\mu \leq 2 - 4 \times 10^{-9}$.⁵

In the next step, we attempt to find the parameter space points that can also solve the $B \rightarrow K^{(*)}\mu\mu$ anomaly by contributing to the $C_{9(10)}$, and at the same time satisfy all the constraints of the LFVs and FCNCs. Since the number of parameters is getting more and more, we are content with a benchmark point that we obtained in the first step. We prepare the benchmark point for the masses to fix the three-loop neutrino function F_{III} ⁶ as follows:

$$M_X \approx 54.26 [\text{GeV}], \quad m_{\eta_I} \approx m_{\eta^\pm} \approx 84.57 [\text{GeV}], \tag{III.3}$$

$$M_1 \approx 277 [\text{GeV}], \quad M_2 \approx 296 [\text{GeV}], \quad M_3 \approx 401 [\text{GeV}], \tag{III.4}$$

$$m_{\Delta_1} \approx 1 [\text{TeV}], \quad m_{\Delta_2} \approx 1.1 [\text{TeV}], \quad m_{\Delta_3} \approx 1.2 [\text{TeV}], \tag{III.5}$$

⁵ In addition to r_{12} , a little bit larger r_{32} is also needed.

⁶ This is technically difficult to obtain the whole numerical values, due to its complicated structure.

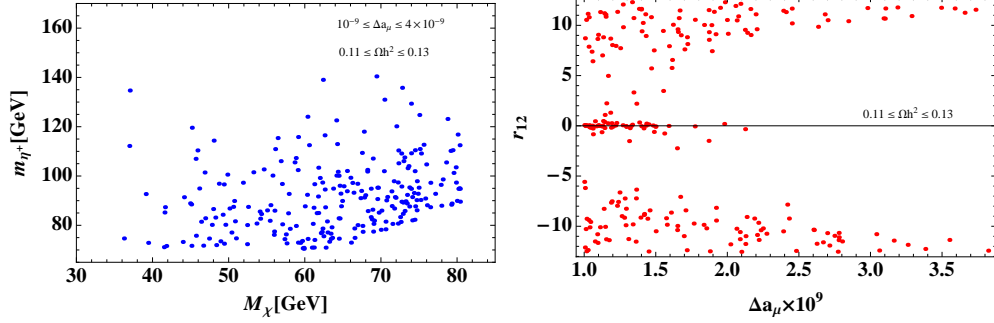


FIG. 2: Scattering plots of the allowed parameter space sets to satisfy LFVs, oblique parameters, and invisible decay of Z boson, in the plane of M_X - m_{η^\pm} in the left panel; and in the plane of Δa_μ - r_{12} in the right panel, where r_{12} is the most relevant parameter to obtain the sizable muon $g-2$ and relic density of DM.

where the above first two lines are provided by the first step so that $\Omega h^2 \approx 0.120$ and $\Delta a_\mu \approx 2.67 \times 10^{-9}$ are obtained with $r_{12} \approx -11.6$. The values in the last line are simply taken to evade the collider bound. To satisfy bound on the direct detection search, $\lambda_3 + \lambda_4 + 2\lambda_5 \lesssim 0.002$ is needed, where experimental upper bound is $\sigma_I \lesssim 2.2 \times 10^{-46} \text{ cm}^2$, while $\lambda_5 \approx 0.035$ that comes from $m_{\eta_I}^2 - M_X^2 = 2\lambda_5 v$. Therefore a little fine tuning is needed among $\lambda_3, \lambda_4, \lambda_5$. With this benchmark point, we have the following values:

$$F_{III}[x_1] \approx -108.68, \quad F_{III}[x_2] \approx -287.73, \quad F_{III}[x_3] \approx -317.11. \quad (\text{III.6})$$

Also, we fix $-\lambda_0 \lambda'_0 v^2 / 2 \approx 1 [\text{GeV}^2]$ for simplicity. Then, we prepare *0.1 billion* random sampling points for the following relevant input parameters:

$$[a_{12}, a_{13}, a_{23}] \in [-1-i, 1+i] \times [10^{-3}, 1], \quad f' \in [-3, \ln(4\pi)], \quad h' \in [-3, \ln(4\pi)], \quad (\text{III.7})$$

where we define $f(h)_{ij} \equiv (\pm 1) \times 10^{f'(h')_{ij}}$. In these parameter ranges, we have found *870* allowed points shown in Fig. 3, which satisfy all the constraints as discussed before. If we focus on the best-fit value of C_9 , these figures show that the Yukawa couplings $f_{1j} (j = 1-3)$ are very restricted as

$$|f_{11}| \lesssim 0.1, \quad |f_{12}| \lesssim 0.02, \quad |f_{13}| \lesssim 0.2, \quad (\text{III.8})$$

where these coupling may affect the collider physics.

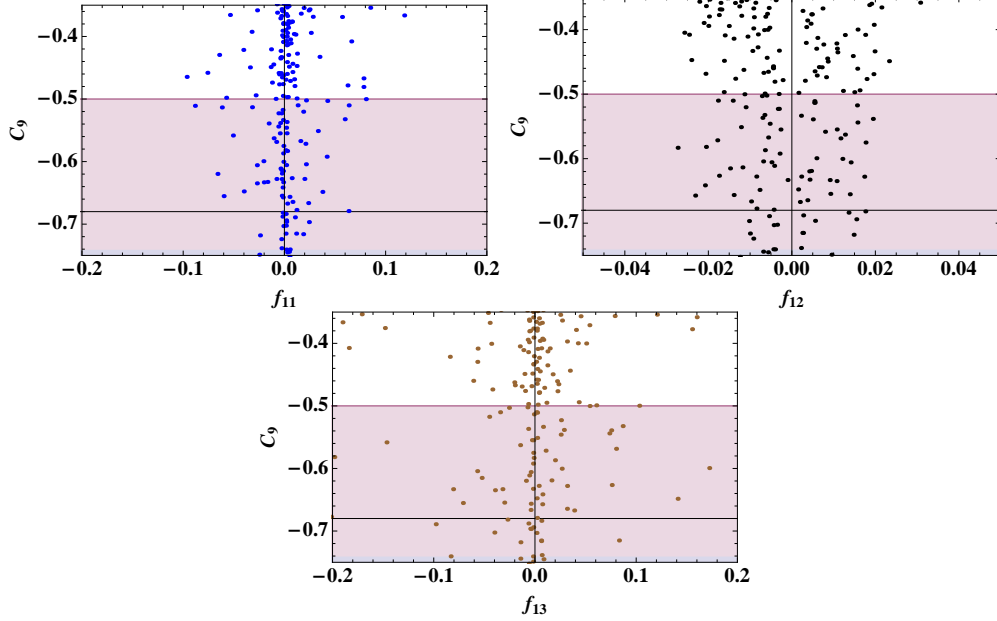


FIG. 3: Scattering plots of the allowed parameter space sets in the plane of $(f_{1j})(j = 1 - 3)-C_9$, where the horizontal line is the best fit value of $C_9 = -0.68$. While the thin red region $[-0.85, -0.50]$ is the one at 1σ range. Notice here that we have taken the range $C_9 \in [-0.75, -0.50]$ to satisfy R_K at 1σ confidential level [3].

Collider Phenomenology: There are two types of new particles in this model other than the SM particles: leptoquarks $\Delta_{1,2,3}^a$ and a set of scalar bosons $\eta^{\pm,0}$ resulting from an isodoublet scalar field.

Note that $\Delta_{1,2}^a$ are assigned with $Z_2 = -1$ while Δ_3^a are assigned with $Z_2 = +1$. All $\Delta_{1,2,3}$ can be pair produced at hadronic colliders and being searched at the LHC. The direct search bound is roughly 1 TeV [26]. On the other hand, only Δ_3^a can participate in the 4-fermion contact interaction, because of the Z_2 parity. The bound from the 4-fermion contact interaction was worked out in Ref. [8, 13] that the bound is currently inferior to the direct search bound of about 1 TeV. Therefore, we shall use 1 TeV as the current bound on the $\Delta_{1,2,3}$ bosons.

The isodoublet field η gives rise to a pair of charged bosons η^\pm , a scalar η_R , and a pseudoscalar η_I . The charged bosons η^\pm can run in the triangular loop vertex of $H\gamma\gamma$. Nevertheless, we can suppress such effects by choosing the λ_5 term in Eq. (II.1) very small. As we have explained above such a term is small to avoid the conflict of the direct detection

bound. Although the interaction between the η field and the SM Higgs field is suppressed for the above reasons, the η can still interact through the kinetic term as it has $SU(2)_L$ and $U(1)_Y$ interactions. We expect some typical interactions with the gauge bosons:

$$Z\eta^+\eta^-, \quad Z\eta_R\eta_I, \quad W^+\eta^-\eta_R, \quad \text{etc.}$$

An interesting signature would be Drell-Yan type production of $\eta^\pm\eta_R$ via a virtual W . The η^\pm decays into multi-leptons and η_R via the virtual L' fields. Therefore, the final state consists of multi-charged-leptons and missing energies. Similarly, in the process $pp \rightarrow Z^* \rightarrow \eta_R\eta_I$, the η_I would decay into η_R eventually with a number of very soft leptons, which may not be detectable. Therefore, the best would be the one produced via virtual W .

IV. CONCLUSIONS

We have investigated a three-loop neutrino mass model with some leptoquark scalars with $SU(2)_L$ -triplet, in which we have explained the anomaly in $B \rightarrow K^{(*)}\mu^+\mu^-$, sizable muon $g-2$, bosonic dark matter, satisfying all the constraints such as LFVs, FCNCs, invisible decay, and so on. Then we have performed the global numerical analysis and shown the allowed region, in which we have found restricted parameter space, *e.g.*,

$$25[\text{GeV}] \lesssim M_X \lesssim 80[\text{GeV}], \quad 70[\text{GeV}] \lesssim m_{\eta^\pm} \lesssim 140[\text{GeV}], \\ |f_{11}| \lesssim 0.1, \quad |f_{12}| \lesssim 0.02, \quad |f_{13}| \lesssim 0.2.$$

We find that $\sim O(100)$ GeV inert doublet scalar is preferred to obtain sizable muon $g-2$. Thus these light inert scalars could be tested by collider experiments such as LHC in which these scalars are produced via electroweak processes. The promising signature of our model comes from the process $pp \rightarrow W^\pm \rightarrow \eta^\pm\eta_R$ which provides signals of multi-leptons plus missing transverse momentum.

Acknowledgments

This work was supported by the Ministry of Science and Technology of Taiwan under Grants No. MOST-105-2112-M-007-028-MY3.

Appendix A: Loop function

Here we show the explicit form of three-loop function F_{III} , which is given by

$$F_{III} = \int [dx_i] \frac{\delta(\sum_{i=1}^5 x_i - 1)(x_2 - 1)^2}{x_1^2} \int \frac{[dy_i] \delta(\sum_{i=1}^3 y_i - 1)}{[(1 + y_1)x_1x_2 - x_1 - x_2 + 1]^3} \int \frac{[dz_i] \delta(\sum_{i=1}^3 z_i - 1)z_1^2}{[y_1\Delta_3 + z_2r_{\delta_{13}^{(2)}} + z_3r_{d_a}]^3},$$

$$\Delta_3 = \frac{x_2 - 1}{x_1[(1 + y_1)x_1x_2 - x_1 - x_2 + 1]} \left(x_1r_{\delta_{13}^{(1)}} + x_2r_{\delta_{13}^{(2)}} + x_3r_b + x_4r_{\eta_R} + x_5r_{\eta_I} \right)$$

$$- \frac{x_1x_2}{A^2y_1[(1 + y_1)x_1x_2 - x_1 - x_2 + 1]} \left(y_2r_{\delta_{13}^{(3)}} + y_3r_{d_c} \right),$$

where $A \equiv x_1/(x_2 - 1)$, $[dx_i] \equiv \int_0^1 dx_1 \int_0^{1-x_1} dx_2 \int_0^{1-x_1-x_2} dx_3 \int_0^{1-x_1-x_2-x_3} dx_4$, $[dy_i] \equiv \int_0^1 dy_1 \int_0^{1-y_1} dy_2$, and $[dz_i] \equiv \int_0^1 dz_1 \int_0^{1-z_1} dz_2$.

-
- [1] R. Aaij *et al.* [LHCb Collaboration], Phys. Rev. Lett. **113**, 151601 (2014) [arXiv:1406.6482 [hep-ex]].
 - [2] R. Aaij *et al.* [LHCb Collaboration], Phys. Rev. Lett. **111**, 191801 (2013) [arXiv:1308.1707 [hep-ex]].
 - [3] S. Descotes-Genon, L. Hofer, J. Matias and J. Virto, JHEP **1606**, 092 (2016) [arXiv:1510.04239 [hep-ph]].
 - [4] G. Hiller and M. Schmaltz, Phys. Rev. D **90**, 054014 (2014) [arXiv:1408.1627 [hep-ph]].
 - [5] G. Hiller, D. Loose and K. Schonwald, JHEP **1612**, 027 (2016) [arXiv:1609.08895 [hep-ph]].
 - [6] S. Descotes-Genon, J. Matias and J. Virto, Phys. Rev. D **88**, 074002 (2013) [arXiv:1307.5683 [hep-ph]].
 - [7] K.A. Olive et al. (Particle Data Group), Chin. Phys. C, **38**, 090001 (2014) and 2015 update.
 - [8] K. Cheung, T. Nomura and H. Okada, arXiv:1610.02322 [hep-ph].
 - [9] L. M. Krauss, S. Nasri and M. Trodden, Phys. Rev. D **67**, 085002 (2003) [arXiv:hep-ph/0210389].
 - [10] M. Aoki, S. Kanemura and O. Seto, Phys. Rev. Lett. **102**, 051805 (2009) [arXiv:0807.0361].
 - [11] M. Gustafsson, J. M. No and M. A. Rivera, Phys. Rev. Lett. **110**, 211802 (2013) arXiv:1212.4806 [hep-ph].
 - [12] C. S. Chen, K. L. McDonald and S. Nasri, Phys. Lett. B **734**, 388 (2014) [arXiv:1404.6033 [hep-ph]].

- [13] K. Cheung, T. Nomura and H. Okada, arXiv:1610.04986 [hep-ph].
- [14] R. Barbieri, L. J. Hall and V. S. Rychkov, Phys. Rev. D **74**, 015007 (2006) [hep-ph/0603188].
- [15] H. Okada and Y. Orikasa, Phys. Rev. D **94**, no. 5, 055002 (2016) [arXiv:1512.06687 [hep-ph]].
- [16] J. P. Lees *et al.* [BaBar Collaboration], Phys. Rev. D **86**, 052012 (2012) [arXiv:1207.2520 [hep-ex]].
- [17] A. M. Baldini *et al.* [MEG Collaboration], arXiv:1605.05081 [hep-ex].
- [18] J. Adam *et al.* [MEG Collaboration], Phys. Rev. Lett. **110**, 201801 (2013) [arXiv:1303.0754 [hep-ex]].
- [19] Review by A. Hoecker and W.J. Marciano in PDG.
- [20] D. S. Akerib *et al.*, arXiv:1608.07648 [astro-ph.CO].
- [21] S. Baek, T. Nomura and H. Okada, Phys. Lett. B **759**, 91 (2016) [arXiv:1604.03738 [hep-ph]].
- [22] T. Hambye, F.-S. Ling, L. Lopez Honorez and J. Rocher, JHEP **0907**, 090 (2009) Erratum: [JHEP **1005**, 066 (2010)] [arXiv:0903.4010 [hep-ph]].
- [23] P. A. R. Ade *et al.* [Planck Collaboration], Astron. Astrophys. **571**, A16 (2014) [arXiv:1303.5076 [astro-ph.CO]].
- [24] P. Osland, A. Pukhov, G. M. Pruna and M. Purmohammadi, JHEP **1304**, 040 (2013) [arXiv:1302.3713 [hep-ph]].
- [25] A. G. Akeroyd *et al.*, arXiv:1607.01320 [hep-ph].
- [26] See for example, M. Aaboud *et al.* [ATLAS Collaboration], New J. Phys. **18**, no. 9, 093016 (2016) [arXiv:1605.06035 [hep-ex]].